The carbon analogues of type-I silicon clathrates

2001 J. Phys.: Condens. Matter 13 5981

(http://iopscience.iop.org/0953-8984/13/26/313)

INSTITUTE OF PHYSICS PUBLISHING JOURNAL OF PHYSICS: CONDENSED MATTER

J. Phys.: Condens. Matter **13** (2001) 5981–5998 www.iop.org/Journals/cm PII: S0953-8984(01)20871-6

The carbon analogues of type-I silicon clathrates

C A Perottoni[1] **and J A H da Jornada**

INMETRO, Avenida N Sra das Graças, 50-Xerém, 25250-020, Duque de Caxias, RJ, Brazil
and
Universidade Federal do Rio Grande do Sul, Instituto de Física, 91501-970 Porto Alegre, RS, Brazil

E-mail: perott@if.ufrgs.br (C A Perottoni)

Received 12 January 2001, in final form 1 March 2001

Abstract

In this paper we present a survey on the structure and equation of state for some silicon clathrates and their carbon analogues, as obtained by means of *ab initio* calculations within the Hartree–Fock approximation. We restrict our consideration to type-I clathrates, namely $M_x(Si, C)_{46}$, with M = Na, Ba. The insertion of guest species into the carbon clathrate cages promotes a significant increase in the host volume, thus reducing the bulk modulus for these compounds. In spite of that, the estimated hardness for C_{46}, of about 61 GPa, constitutes an exceptionally large value for a structure with such an open framework. The issue of electronic charge transference from the guest species to the host framework and the stability of carbon and silicon clathrates relative to the diamond phase are also discussed.

1. Introduction

The clathrates constitute a class of inclusion compounds composed by two or more chemical species, in which some of them (the guest species) are caged by the host tridimensional framework formed by the others [1–4]. The name clathrate came from the Latin word *clathratus*, which means 'enclosed or protected by cross bars of a grating' [1].

The earliest observations of such compounds date back to the 19th century, from the studies of Davy on chlorine hydrates. The ability of clathrate compounds to entrap guest species was already described by Mylius, as early as 1886, who observed this peculiar behaviour in hydroquinone complexes [2].

In spite of the fact that several chemical properties of clathrate compounds were already known of early in the 19th century, their understanding in terms of an accurate description of their crystal structures only began to be attained sixty years after the work of Mylius [4]. Among the first clathrates whose crystal structures were solved are the cubic gas hydrates, known as type-I clathrates [3, 4]. The general stoichiometric formula of these compounds

[1] Author to whom any correspondence should be addressed, at Universidade Federal do Rio Grande do Sul, Instituto de Física, 91501-970 Porto Alegre, RS, Brazil.

0953-8984/01/265981+18$30.00

is $M_x{\cdot}46H_2O$ ($x \leqslant 8$), where M is a guest species that is gaseous at ambient conditions. The crystalline framework of these gas hydrates is composed by water molecules linked by hydrogen bonds. Besides gas hydrates, water also forms other clathrate hydrates, including $M_x{\cdot}136H_2O$ compounds, known as liquid hydrates, or type-II clathrates [3, 4].

In the course of a systematic study on the thermal decomposition of the Zintl phase sodium silicide (NaSi), Cros *et al* prepared, thirty-five years ago, a cubic compound of sodium and silicon, isostructural to gas hydrates [5,6]. In the years that followed that first discovery, several type-I and type-II clathrates of group-14 elements were prepared, with group-1 and group-2 elements as templating guest species.

The crystal structure of type-I silicon clathrates (space group $Pm\bar{3}n$, $Z = 1$) can be described as a tridimensional framework of four-coordinated silicon atoms, disposed in space so as to form two kinds of polyhedron (see figure 1): a pentagonal dodecahedron, Si_{20}, composed of twelve pentagonal faces, and a tetrakaidecahedron, Si_{24}, with twelve pentagonal and two hexagonal faces. The type-I clathrate framework is thus made of a tridimensional arrangement of these face-sharing polyhedra. The space inside the Si_{20} and Si_{24} cages can be filled with guest species of suitable size, including various group-1 and group-2 elements from the periodic table.

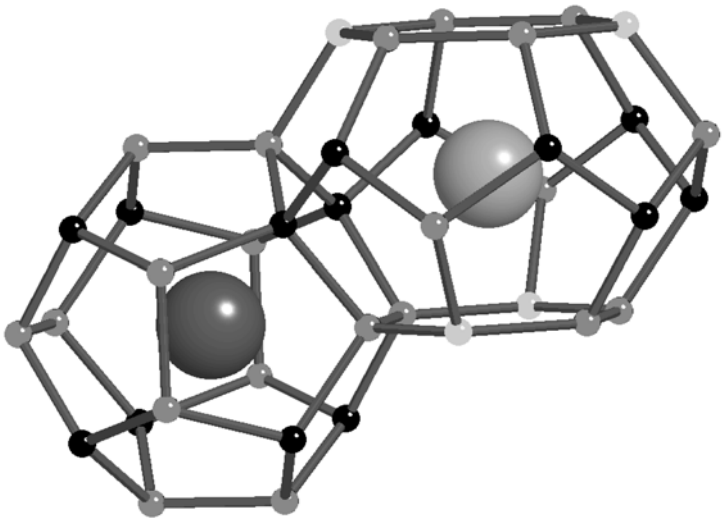

Figure 1. Detail of the type-I Na_8Si_{46} clathrate structure, showing the distinct site positions and the silicon polyhedra: the pentagonal dodecahedron, on the left, and the tetrakaidecahedron, on the right. The silicon atoms occupying the sites 6c (Si(1)), 16i (Si(2)), and 24k (Si(3)) of the space group $Pm\bar{3}n$, in the clathrate framework, are represented by the small light-, dark-, and medium-grey spheres, respectively. The large dark- and light-grey spheres represent the guest sodium atoms at the crystallographic sites 2a (Na(1)) and 6d (Na(2)), respectively.

Silicon and germanium clathrate compounds exhibit very interesting physical properties. Recently, Kawaji *et al* [7] found that $(Na, Ba)_xSi_{46}$ becomes a superconductor below 4 K. This discovery drew attention to this compound, not because of the critical temperature for the onset of the superconductor state, which is rather low, but mainly because it constitutes the first example of a superconductor consisting of a silicon sp^3 framework. Since this first report, superconductivity has been found among other group-14 clathrates, including $(Ba, K)_xSi_{46}$ [8] and mixed clathrates such as $Ba_8Ga_{16}Ge_{30}$ [9]. As another example of

the interesting properties exhibited by these compounds, consider the transport properties of group-14 clathrates. As a general rule, the guest species in clathrate compounds are loosely bound to the covalent framework. As the guest atoms rattle inside the clathrate cages, they scatter thermal phonons incoherently, thus reducing the thermal conductivity significantly. The reduced thermal conductivity, together with the metallic-like electrical conductivity of some silicon and germanium clathrates, makes them promising candidates for thermoelectric applications [10–15].

The carbon analogues of silicon clathrates are expected to exhibit even more astonishing physical properties. For instance, Benedek *et al* [16] suggested that a type-I carbon compound analogous to the silicon clathrate $Na_2Ba_6Si_{46}$, first synthesized by Yamanaka *et al* [17], could exhibit a bulk modulus about 15% higher than that of diamond. Such 'metallic diamonds' [18] are also potential high-T_c superconductors, owing to the extreme rigidity of the covalent carbon framework (that leads to a high Debye temperature), high density of states near the Fermi level, and strong electron–phonon coupling. Recent results obtained from studies of an almost empty type-II silicon clathrate also suggest that analogous compounds made up by carbon atoms would be made extremely hard, possibly even harder than diamond, by appropriate introduction of guest species into the framework cages [19]. The low compressibility, high hardness, and the prospect of superconductivity with a high T_c make carbon clathrates very interesting compounds both from the point of view of basic science and also because of their great promise for technological applications. However, thirty-five years after the discovery of a synthetic route for obtaining silicon clathrates, there is still no reported successful synthesis of an analogous carbon compound.

Previous work dealing with *ab initio* or semi-empirical calculations on type-I silicon and carbon clathrates was mainly devoted to the study of their energetics, electronic structure, or vibrational properties [18–29]. Early papers reporting calculations on the equation of state of type-I clathrates concern only the pressure behaviour of empty-cage silicon (or carbon) clathrates [22–27]. In this paper, we present a detailed, systematic comparison between the structure and equation of state for some silicon clathrates and their carbon analogues, as obtained from *ab initio* calculations at the Hartree–Fock level. We restrict the scope of the present paper to type-I clathrates, including Na_8Si_{46}, the empty-cage compound Si_{46}, their carbon analogues, and $Na_2Ba_6C_{46}$, as well as silicon and carbon in the diamond structure. After a brief description of the computational procedure employed in this work, we describe the effects on the structure and equation of state for the empty clathrates resulting after substituting carbon for silicon in the covalent framework, and also after the insertion of guest atoms into the clathrate cages. The paper proceeds by discussing the stability of carbon clathrates relative to the diamond phase, and addressing the issue of electronic charge transfer from the guest species to the host framework. One of our aims in this work is to verify to what extent previous assumptions about the extreme hardness expected for some carbon clathrates are supported by *ab initio* calculations. Accordingly, from the calculated elastic constants for C_{46}, we estimate its hardness by means of a correlation proposed by Clerc for diamond-like materials [30]. We also estimated the Debye temperature for C_{46}, a quantity closely related to the critical temperature for the transition to the superconducting state. The paper ends with some thoughts on the more suitable choices for the chemical species that could act as templates for the synthesis of carbon clathrates.

2. Computational details

The calculations described in this paper were performed within the all-electron Hartree–Fock approximation, in the athermal limit, with the CRYSTAL95 computer code [31]. The crystal

wavefunction was expanded in a basis formed by a linear combination of crystalline orbitals (HF-LCCO approximation). The crystalline orbitals were each expressed as a sum over all equivalent sites in the periodic system of atomic-centred Gaussian functions. For the evaluation of enthalpy differences and transition pressures between clathrate and diamond phases, the binding energies were corrected, *a posteriori*, for the inclusion of correlation effects, according to the density functional approximation, with the Perdew–Burke–Ernzerhof functional [32]. In this work, we employed standard 6-21G and 6-21G* split valence basis sets for both carbon and silicon [33, 34]. The carbon and silicon outer-valence Gaussian exponents (α_{sp}) were optimized by minimizing the total energy for C_2 and Si_2 (carbon and silicon with the diamond structure, respectively). This procedure yielded $\alpha_{sp} = 0.226$ for carbon and $\alpha_{sp} = 0.115$ for silicon. The 6-21G* basis was constructed by adding a d-like Gaussian orbital to the 6-21G basis, with exponents $\alpha_d = 0.8$ and $\alpha_d = 0.55$ for carbon and silicon, respectively. The sodium and barium basis sets were adapted from references [35] and [36], respectively. The sodium and barium outermost-valence-shell exponents and coefficients were optimized, minimizing the total energy for the hypothetical compound $Na_2Ba_6C_{46}$. The optimization was done in two steps. First, with the original basis sets for Na and Ba taken from the literature, we performed a preliminary optimization of the crystal structure of the $Na_2Ba_6C_{46}$ clathrate. The Na and Ba basis sets were then optimized, keeping the lattice parameter and atomic positions as found in the first step constant. The optimized basis set for Ba and Na are given in table 1 and table 2, respectively.

With the exception of the binding energies, the physical properties reported in this paper were obtained from calculations performed with the following tolerances (in atomic units) for the evaluation of the infinite Coulomb and exchange series [31]: 10^{-8} for the exchange overlap, Coulomb overlap, Coulomb penetration, and the first exchange pseudo-overlap; and 10^{-14} for the second exchange pseudo-overlap tolerance. The Fock matrix has been diagonalized at a number of $\boldsymbol{k}$-points, within the irreducible Brillouin zone (IBZ), corresponding to a shrinkage factor of 8 in the Monkhorst–Pack net [37]. Owing to the metallic character of some of these clathrates, a dense Gilat net [38] was defined with a shrinkage factor of 16. To reduce the numerical noise, for each compound all of the calculations were performed keeping the same set of indexed bielectronic integrals selected from a reference geometry [31]. For the calculation of binding energies, very tight cut-offs were selected for the evaluation of the infinite Coulomb and exchange series: 10^{-12} for the exchange overlap, Coulomb overlap, Coulomb penetration, and the first exchange pseudo-overlap; and 10^{-18} for the second exchange pseudo-overlap tolerance. For carbon in the diamond structure (C_2), a further reduction in the above-defined cut-offs for the evaluation of bielectronic integrals, as well as an increase in the shrinkage factors that define the Monkhorst–Pack and Gilat nets, resulted in changes in the binding energy smaller than 0.01 mHartree.

3. Results and discussion

3.1. Crystal structure and equation of state

Type-I silicon (carbon) clathrates contain 46 atoms of silicon (carbon) per primitive cell, plus the metal atoms. Their crystal structure can be fully described by a set of four parameters, namely the lattice parameter (a_0) and three free parameters defining the silicon (carbon) position in the sites 16i (x, x, x) and 24k $(0, y, z)$ of space group $Pm\bar{3}n$ (see figure 1). Consequently, in the athermal limit, the optimized structure of these type-I clathrates can be found by minimizing the static energy E:

$$E = E(a_0, x, y, z). \tag{1}$$

Table 1. The barium basis set. Exponents (in au) and s, p, and d coefficients of the barium-centred Gaussian basis set, as optimized in $Na_2Ba_6C_{46}$.

		Coefficients		
Type	Exponent	s	p	d
s	5268534.5000000	0.0000487		
	770380.7500000	0.0003990		
	165754.0000000	0.0023100		
	43022.7000000	0.0111000		
	12502.3880000	0.0460000		
	3992.6684000	0.1534000		
	1421.8082000	0.3477000		
	567.1226000	0.4330000		
	238.9643100	0.2053000		
sp	15454.3160000	−0.0003780	0.0011000	
	3602.2466000	−0.0063600	0.0099200	
	1118.0562300	−0.0517000	0.0574000	
	403.4250400	−0.1463000	0.2166000	
	165.6381200	0.0839000	0.4578000	
	77.5693800	0.6077000	0.4717000	
	38.1557800	0.5106000	0.2341000	
sp	387.6657400	0.0062500	−0.0124000	
	146.1260500	−0.0215000	−0.0742000	
	59.6066400	−0.3106000	−0.0032900	
	27.2402200	−0.0856000	0.8572000	
	13.0831500	0.9117000	1.3915000	
	6.4982900	0.5540000	0.5311000	
d	436.9040000			0.0151000
	130.4980000			0.1041000
	49.0975000			0.3255000
	20.5988000			0.4708000
	9.4682000			0.2707000
	4.5895000			0.0473000
sp	9.9542000	0.5334000	−0.1412000	
	6.4094000	0.1985000	0.2844000	
	3.2089000	0.0769000	0.2868000	
d	8.4525000			0.2177000
	3.4646000			0.5783000
	1.4564000			0.4139000
d	0.2000000			1.0000000
sp	5.1897000	0.1873000	0.2803000	
	2.3702000	0.9590000	1.3841000	
	1.1730000	0.4417000	0.6019000	
sp	0.3377000	1.0000000	1.0000000	
sp	1.0050000	1.0000000	1.0000000	

The high computational cost of performing *ab initio* calculations with so great a number of atoms per primitive cell makes unfeasible the minimization of (1) with carbon/silicon 6-21G* basis sets. Consequently, the atomic positions were optimized with carbon/silicon 6-21G basis sets and then kept fixed in the remaining calculations.

Table 2. The sodium basis set. Exponents (in au) and s and p coefficients of the sodium-centred Gaussian basis set, as optimized in $Na_2Ba_6C_{46}$.

		Coefficients	
Type	Exponent	s	p
s	56700.0000000	0.0002250	
	8060.0000000	0.0019100	
	1704.0000000	0.0110500	
	443.6000000	0.0500600	
	133.1000000	0.1691000	
	45.8000000	0.3658000	
	17.7500000	0.3998000	
	7.3800000	0.1494000	
sp	119.0000000	−0.0067300	0.0080300
	25.3300000	−0.0798000	0.0639000
	7.8000000	−0.0793000	0.2074000
	3.0000000	0.3056000	0.3398000
	1.2890000	0.5639000	0.3726000
sp	0.5843000	1.0000000	1.0000000
sp	0.3218000	1.0000000	1.0000000

The parameters obtained by minimizing the above expression for some silicon clathrates, and their carbon analogues, are summarized in table 3. The optimized crystal structures of the type-I silicon and carbon clathrates studied in this work are depicted in figure 2. The interatomic distances and angles for the optimized structures are given in table 4 for the silicon clathrates and in table 5 for their carbon analogues.

Table 3. Structural parameters for the carbon and silicon clathrates studied in this work, as obtained by minimizing expression (1), at the HF-LCCO level of theory, with the standard 6-21G basis set for carbon and silicon. The last row includes experimental data for Na_8Si_{46}, as taken from reference [6].

Compound	a_0 (Å)	16i $(x, x, x) - x$	24k $(0, y, z) - y$	24k $(0, y, z) - z$
C_{46}	6.700	0.1845	0.3055	0.1190
Na_8C_{46}	6.967	0.1876	0.3049	0.1245
$Na_2Ba_6C_{46}$	7.655	0.1878	0.2973	0.1589
Si_{46}	10.406	0.1839	0.3070	0.1176
Na_8Si_{46}	10.19	0.183	0.31	0.116

As can be seen in figure 2, substituting carbon for silicon in the clathrate framework leads to a substantial decrease of the lattice cell volume. In fact, according to our results, the C_{46} lattice parameter amounts to only about 64% of that of Si_{46}. This lattice shrinkage represents a fourfold reduction in the C_{46} molar volume relative to Si_{46}. This is about the same volume contraction as was found in comparing the molar volume for silicon and carbon, both with the diamond structure.

This lattice shrinkage makes it difficult to accommodate large guest species inside the cages of carbon clathrates. For instance, the inclusion of sodium into C_{46}, leading to Na_8C_{46}, is accompanied by an increase of 4% in the lattice parameter. According to our results, no such volume increase is observed in going from Si_{46} to Na_8Si_{46}. Substituting barium for sodium into the two larger cages (C_{24}) of the carbon clathrate structure results in large strains of the framework C–C bonds, mainly for the C(3)–C(3) bond, which eventually broke, as shown in

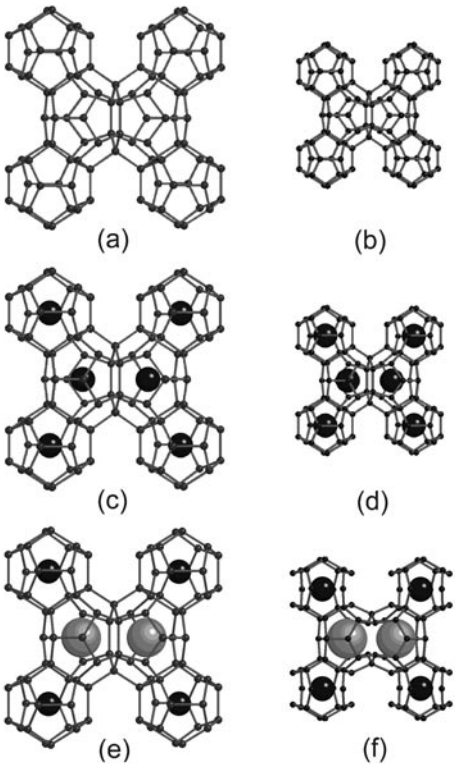

Figure 2. A schematic representation of the crystal structures of the silicon clathrates (on the left) and their carbon analogues (on the right), as optimized within the HF-LCCO approximation. Represented in this figure are the clathrates (a) Si_{46}, (b) C_{46}, (c) Na_8Si_{46}, (d) Na_8C_{46}, (e) $Na_2Ba_6Si_{46}$ [17], and (f) $Na_2Ba_6C_{46}$. The small spheres represent silicon (carbon) atoms from the host framework, and the large dark- and light-grey spheres represent sodium and barium guest atoms, respectively.

figure 2(f). Indeed, for $Na_2Ba_6C_{46}$, the C(3)–C(3) distance is about twice the largest known C_{sp^3}–C_{sp^3} bond length in hydrocarbons, namely 1.720(4) Å [39].

The average C–C bond length for the carbon clathrates studied in this work is 1.56(2) Å, 1.61(6) Å, and 1.76(25) Å for C_{46}, Na_8C_{46}, and $Na_2Ba_6C_{46}$, respectively. The figures quoted in parentheses represent the standard deviations for the set of C–C bond lengths calculated for these type-I clathrates. The average bond-length standard deviation is far greater for $Na_2Ba_6C_{46}$, mainly due to the abnormally large C(3)–C(3) bond length resulting upon barium insertion. Relative to the C–C bond length in diamond ($d_{C-C} = 1.5446$ Å), the above values for the average bond lengths in carbon clathrates represent an increase of 0.7% for the empty-cage clathrate C_{46}, and about 4% and 14% for Na_8C_{46} and $Na_2Ba_6C_{46}$, respectively. The average Si–Si bond length in the silicon clathrates Si_{46} and Na_8Si_{46} is 2.39(2) Å and 2.384(2) Å, respectively[2]. Relative to silicon diamond, the average Si–Si bond length in Si_{46} and Na_8Si_{46} increases by about 1.5%.

The analysis of the C–C bond lengths in Na_8C_{46}, particularly the C(3)–C(3) bond, reveals that the insertion of sodium into C_{46} cages brings this clathrate close to the threshold of C–C

[2] The Si–Si distances in Na_8Si_{46} were calculated using the experimental atomic positions [6] and the lattice parameter as optimized at the Hartree–Fock level.

Table 4. Interatomic distances and angles for silicon clathrates Na_8Si_{46} (experimental [6] and theoretical) and Si_{46}, as obtained from the crystal structures optimized at the HF-LCCO level (see the text for details). For comparison, the experimental Si–Si distance in silicon diamond (Si_2) is 2.3516 Å.

A–B distance (Å)	Na_8Si_{46} (experiment)	Na_8Si_{46} (HF)	Si_{46}
Si(1)–Si(3)	2.369	2.385	2.404
Si(2)–Si(2)	2.365	2.381	2.352
Si(2)–Si(3)	2.370	2.386	2.373
Si(3)–Si(3)	2.364	2.380	2.416
Na(1)–Si(2)	3.223	3.252	
Na(1)–Si(3)	3.372	3.396	
Na(2)–Si(1)	3.603	3.627	
Na(2)–Si(2)	3.792	3.818	
Na(2)–Si(3)	3.960	3.988	
Na(2)–Si(3)	3.411	3.434	
Angle $A\widehat{B}C$ (deg)	Na_8Si_{46} (experiment)	Na_8Si_{46} (HF)	Si_{46}
Si(3)–Si(1)–Si(3)	109.6	109.6	111.1
Si(3)–Si(1)–Si(3)	109.4	109.4	108.7
Si(2)–Si(2)–Si(3)	107.8	107.8	108.5
Si(3)–Si(2)–Si(3)	111.1	111.1	110.4
Si(2)–Si(3)–Si(2)	103.8	103.8	105.5
Si(2)–Si(3)–Si(1)	106.3	106.3	106.1
Si(2)–Si(3)–Si(3)	106.7	106.7	106.7
Si(1)–Si(3)–Si(3)	125.2	125.2	124.4

bond rupture (as can be inferred from the comparison with the largest C_{sp^3}–C_{sp^3} bond length ever found, already commented on above). The resulting large strains in the covalent framework C–C bonds increase considerably the binding energy of Na_8C_{46} relative to the empty carbon clathrate. The smaller 'free space' available inside the cages in carbon clathrates, relative to their silicon analogues, in fact precludes the insertion of large cations such as barium, which can be accomplished only with a great expansion of the cubic cell volume and rupture of the carbon framework.

With the atomic positions kept fixed at their optimized values as given in table 3, the clathrate lattice parameter was varied in order to obtain the volume dependence of the total energy. In these calculations we employed both the 6-21G and 6-21G* basis sets for carbon and silicon. A Murnaghan equation of state [40] was fitted to the energy versus volume data, yielding the equilibrium lattice parameter and bulk modulus for the silicon and carbon clathrates, as quoted in table 6. The lattice parameters resulting from the fitting of the Murnaghan equation of state to the data obtained with C/Si 6-21G basis sets compares well with those obtained by minimizing (1), with the same basis set, thus serving as a cross-check of our calculations.

As can be seem in table 6, the inclusion of a polarization function to form the 6-21G* basis sets yields smaller lattice parameters (as compared to those found in the calculations with C/Si 6-21G basis sets), that also compare better with the available experimental results. This effect was already observed in early crystalline and molecular calculations, where the inclusion of polarization (d-like) orbitals almost always reduces bond lengths [44]. The bulk

Table 5. Interatomic distances and angles for carbon clathrates C_{46}, Na_8C_{46}, and $Na_2Ba_6C_{46}$, as obtained from the crystal structures optimized at the HF-LCCO level (see the text for details). For comparison, the experimental C–C distance in diamond (C_2) is 1.5446 Å.

A–B distance (Å)	C_{46}	Na_8C_{46}	$Na_2Ba_6C_{46}$
C(1)–C(3)	1.569	1.614	1.695
C(2)–C(2)	1.518	1.504	1.643
C(2)–C(3)	1.540	1.601	1.672
C(3)–C(3)	1.592	1.733	2.423
Na(1)–C(2)		2.261	2.480
Na(1)–C(3)		2.292	2.570
Na(2)/Ba–C(1)		2.460	2.696
Na(2)/Ba–C(2)		2.573	2.818
Na(2)/Ba–C(3)		2.641	2.626
Na(2)/Ba–C(3)		2.371	2.737
Angle $A\widehat{B}C$ (deg)	C_{46}	Na_8C_{46}	$Na_2Ba_6C_{46}$
C(3)–C(1)–C(3)	112.1	114.5	131.6
C(3)–C(1)–C(3)	108.2	107.0	99.67
C(2)–C(2)–C(3)	108.9	109.6	106.4
C(3)–C(2)–C(3)	110.1	109.4	112.4
C(2)–C(3)–C(2)	106.6	109.2	117.8
C(2)–C(3)–C(1)	106.1	106.3	113.7
C(2)–C(3)–C(3)	106.5	105.9	97.57
C(1)–C(3)–C(3)	124.0	122.8	114.2

Table 6. Comparison between the parameters of the Murnaghan equation of state, as obtained at the HF-LCCO level with C/Si 6-21G and 6-21G* basis sets. Quoted in the columns under 'Δ (%)' are the percentage differences between theoretical and experimental values for lattice parameters and bulk modulus. For the calculation of these percentage differences, the experimental results for C_2 were taken from reference [41], for Si_2 from references [42] and [43], and for the Na_8Si_{46} lattice parameter, from reference [6].

	6-21G				6-21G*			
Compound	a_0 (Å)	Δ (%)	B_0 (GPa)	Δ (%)	a_0 (Å)	Δ (%)	B_0 (GPa)	Δ (%)
C_2	3.5737	0.18	454	1.8	3.5695	0.07	467	4.7
C_{46}	6.7029	—	409	—	6.6914	—	425	—
Na_8C_{46}	6.9782	—	358	—	6.9588	—	378	—
$Na_2Ba_6C_{46}$	7.6227	—	245	—	—	—	—	—
Si_2	5.5695	2.6	91	−7.0	5.4919	1.1	109	11
Si_{46}	10.406	—	82	—	10.271	—	96	—
Na_8Si_{46}	10.387	1.9	88		10.260	0.68	101	

modulus calculated with the C/Si 6-21G* basis sets are also higher than that obtained without the polarization function. The comparison with the available experimental results indicates that our calculations follow the usual tendency of HF approximation to overestimate the bulk modulus. Indeed, the bulk moduli obtained from the calculations with C/Si 6-21G* basis sets are greater than the experimental values by 4.7% and 11% for carbon and silicon with the

diamond structure, respectively. The bulk modulus for Na_8Si_{46}, with both silicon 6-21G and 6-21G* basis sets, is slightly lower than the value found for Si_2. It is noteworthy that for none of the clathrates studied in this work was the calculated bulk modulus greater than that of the corresponding diamond structure. Both the volume increase and bond breaking resulting from sodium and barium insertion contribute to significant reduction of the bulk modulus of $Na_2Ba_6C_{46}$, which, according to our calculations, amounts to only about 54% of that of diamond, far lower than the bulk modulus previously estimated by Benedek *et al* for $A_2B_6C_{46}$ clathrates in general [16].

3.2. Enthalpy and phase transitions

Despite the fact that the bulk modulus and the equilibrium volume are, in general, estimated with relative confidence by HF calculations, the same cannot be said about binding energies, because of the lack of any treatment of electronic correlation at this level of theory. This led us to adopt a hybrid procedure [45] for the calculation of the enthalpy (that is equal to the Gibbs free energy in the athermal limit) and pressures of transition between the clathrate and diamond phases. Accordingly, the enthalpy of each phase [45]

$$H(P) = \frac{B_0 V_0}{B_0' - 1}\left[\left(\frac{B_0'}{B_0}P + 1\right)^{1-1/B_0'} - 1\right] + E_0 \tag{2}$$

is evaluated with the values for B_0 and V_0 obtained at the HF level, while the binding energy (E_0) is corrected, *a posteriori*, for the inclusion of electronic correlation. This correction was performed according to the density functional theory (DFT), using the Perdew–Burke–Ernzerhof functional [32]. The binding energies estimated in this way for carbon and silicon in the diamond structure, −7.526 eV and −4.735 eV, respectively, differ by only 0.33% and −0.86% from the experimental binding energies corrected to the athermal limit [44]. The enthalpy difference between clathrate and diamond phases and the estimated pressures for the clathrate → diamond transition, for the compounds studied in this work, are summarized in table 7. The enthalpy–pressure relationship for the different compounds studied in this work is represented in figure 3.

Table 7. Pressures (P_t) for the transition between clathrate and diamond phases. $V_1(P_t)$ and $V_2(P_t)$ represent the volume per atom of carbon or silicon, at the transition pressure, in the clathrate and diamond phases, respectively. In the last column are quoted the differences in enthalpy, at zero pressure, in the athermal limit, of the clathrate phases relative to the diamond structure.

Compound	P_t (GPa)	$V_1(P_t)$ (Å^3/atom)	$V_2(P_t)$ (Å^3/atom)	ΔH_0 (eV/atom)
Si_{46}	−5.95	25.29	22.01	0.113
Na_8Si_{46}	−5.10	24.84	21.80	0.093
C_{46}	−37.3	7.256	6.259	0.210
Na_8C_{46}	−77.1	11.18	7.447	1.077

The enthalpy per atom, at zero pressure (which is equivalent to the binding energy per atom), for the carbon clathrate C_{46}, relative to the diamond phase, $\Delta H_0 = 0.21$ eV, compares well with previous results obtained by O'Keefe *et al* [29] and also by Benedek *et al* [24]. It is noteworthy that the type-I clathrate C_{46} has a binding energy, relative to diamond, which is about half of that of the C_{60} fullerene (0.43 eV/atom) [46].

With the aid of expression (2) it was found that the enthalpy for the diamond and clathrate phases of carbon (C_2 and C_{46}) and silicon (Si_2 and Si_{46}) becomes equal at pressures of $P_t = -37.3$ GPa and $P_t = -5.95$ GPa, respectively (see table 7). These values can be

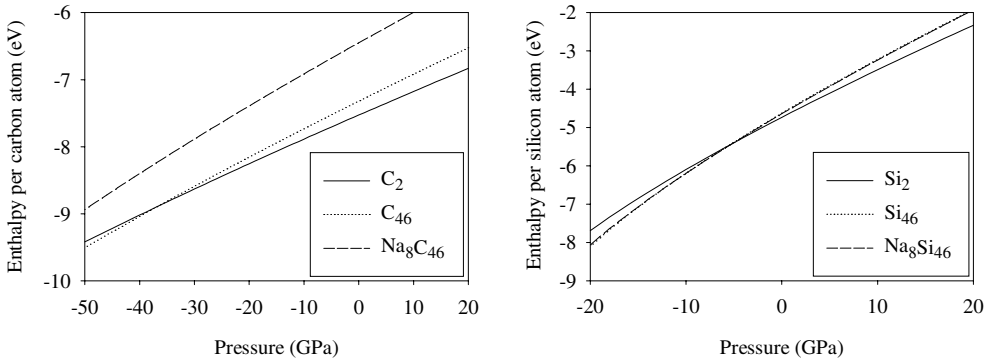

Figure 3. The pressure dependence of enthalpy (2), in the athermal limit, for carbon (on the left) and silicon (on the right) in the diamond and clathrate (with and without sodium inserted as guest atom) structures.

compared with the results obtained by Dong and Sankey [47] for the pressure of the transition $Ge_{46} \rightarrow Ge_2$, $P_t = -2.4$ GPa. The result is that the pressure at which the diamond and clathrate phases are in equilibrium, in the athermal limit, increases (in absolute value) in the sequence Ge $\rightarrow$ Si $\rightarrow$ C. According to our calculations, the transition from $Si_{46} \rightarrow Si_2$ would occur with a volume discontinuity of about -12.9%, while the corresponding transition for their carbon analogue, at -37.3 GPa, would shrink the volume per carbon atom by -13.7%. Without taking into account the small amount of sodium, it can be estimated that the clathrate Na_8C_{46} becomes stable relative to the diamond phase only at very negative pressures of about -77 GPa.

At ambient pressure, the silicon clathrates Si_{46} and Na_8Si_{46} are unstable relative to the diamond phase, Si_2. This by no means precludes the synthesis and metastable retention of Na_8Si_{46}, that converts to silicon diamond only when heated at above 450 °C [5]. Interestingly, San-Miguel *et al* recently reported that type-II clathrate Si_{136} transforms directly to the β-Sn phase of silicon upon compression, and not to the diamond phase, as could be expected [19]. Preliminary results indicate a similar behaviour for the sodium-inserted type-I clathrate Na_8Si_{46} [19]. With the results obtained in this work for Na_8Si_{46}, and with those given by Pandey *et al* [48] for β-Sn silicon, we can estimate a pressure $P_t = 14.2$ GPa for the transition $Na_8Si_{46} \rightarrow \beta$-Sn silicon, in excellent agreement with preliminary results from San-Miguel *et al* [19].

In the athermal limit, the clathrate phase is thermodynamically stable, relative to the diamond structure, only at very negative pressures. Such enormous negative transition pressures represent a challenge to the synthesis of carbon compounds analogous to type-I silicon clathrates, given the significant driving force acting, even at ambient pressure, in the sense of the transition to the diamond phase. For the carbon clathrates studied in this work, these negative pressures are, in absolute value, far greater than the corresponding (positive) pressure for the transition from graphite to diamond. In fact, for carbon at $T = 0$ K, the diamond phase becomes thermodynamically stable, relative to graphite, above about 1.4 GPa [49]. However, the energy barrier for this transition is sufficiently high to prevent the conversion from graphite to diamond, which is only accomplished at pressures in excess of several gigapascals and high temperatures, in the presence of a metal catalyst. Accordingly, we cannot rule out the very possibility of synthesizing carbon clathrates, solely on the basis of the present calculations. A more conclusive answer regarding the synthesis and metastable retention of carbon clathrate compounds under ambient conditions should wait until a better knowledge of the transition barrier between the clathrate and diamond phases becomes available.

3.3. Hardness and Debye temperature of the empty-cage clathrate C_{46}

The hardness of a material is usually referred as a measure of its plastic response to an applied load in an indentation test. Being the result of a physical process more than an intrinsic property, and being also influenced by the sample history and microstructure, hardness is a physical property that is extremely difficult to obtain directly from first-principles calculations. To overcome this limitation, one possibility is to make use of one of the various semi-empirical correlations relating the hardness of a material to its elastic properties, generally the bulk or shear modulus.

Accordingly, the hardness of diamond (C_2) and that of the empty-cage carbon clathrate C_{46} were estimated using a semi-empirical expression proposed by Clerc for AB diamond-like materials [30]:

$$H = 0.0748G\left(1 + \frac{Z_A}{Z_B}\right) \tag{3}$$

which gives the hardness H as a function of the effective nuclear charges Z_A and Z_B, for species A and B, respectively, and the shear modulus, G. This latter is obtained as the arithmetic average of the Hashin–Shtrikman upper and lower bounds for the shear modulus of a quasi-isotropic polycrystal [50, 51].

The three independent elastic constants c_{11}, c_{12}, and c_{44}, for C_2 and C_{46}, used in the evaluation of the Hashin–Shtrikman upper and lower bounds for the shear modulus, are given in table 8. This table also includes the bulk modulus $B = \frac{1}{3}(c_{11} + 2c_{12})$, the arithmetic average of the shear modulus, obtained according to [50, 51], and the hardness estimated from (3) for C_2 and C_{46}. The elastic constants for C_2 and C_{46} were obtained, *ab initio*, by applying conveniently chosen lattice deformations and fitting the resulting dependence of the total energy on the adimensional lattice strain parameter [31]. Table 8 also includes the experimental elastic constants for diamond, as taken from reference [52], as well as the elastic moduli and the hardness estimated from them.

Table 8. Elastic constants (c_{11}, c_{12}, and c_{44}), bulk and shear moduli (B and G), and hardness (H) for carbon clathrate C_{46} and diamond C_2 (both theoretical and experimental). All parameters are quoted in GPa. The experimental elastic constants for diamond, and the values for B, G, and H estimated from them, are included for comparison.

Compound	c_{11}	c_{12}	c_{44}	B	G	H
C_2 (theory)	1237	85	675	469	633	95
C_2 (experiment)	1076	125	576	442	533	80
C_{46}	1149	44	591	412	490	73

The comparison with the experimental values reveals that the shear modulus calculated for diamond, at the Hartree–Fock level, is overestimated by about 19%. Accordingly, the diamond hardness obtained from (3) is also overestimated. Assuming that the correct hardness for diamond is that obtained from (3), with the shear modulus calculated from the experimental elastic constants ($H = 80$ GPa), we obtain a correction factor of $80/95 = 0.84$, which can thus be applied to the theoretically calculated hardness to scale the result found for C_{46}. Even after this scaling procedure, the estimated hardness for C_{46} ($H = 61$ GPa) is almost 25% higher than that of the second-hardest material known to date, namely cubic boron nitride (c-BN), for which $H = 49$ GPa [30, 52]. The hardness estimated for the hypothetical clathrate C_{46} constitutes, indeed, an exceptionally large value for a structure with such an open framework.

From the elastic constants quoted in table 8, the Debye temperature θ_D can be estimated, for C_2 and C_{46}, following the procedure outlined by Anderson [53]. It turns out that the Debye

temperature for C_{46} is about 97% of that for diamond, when the estimate of θ_D is made, for both compounds, from the elastic constants obtained within the Hartree–Fock approximation. According to the BCS theory of superconductivity, the critical temperature (T_c) for the transition to the superconducting state is directly proportional to the Debye temperature. It turns out that, considering solely the effect on the Debye temperature and keeping all other things unchanged, substituting carbon for silicon in the framework of type-I silicon clathrates should promote a sevenfold increase in T_c. In fact, owing to a possibly enhanced electron–phonon coupling [18], one can expect an even greater increase in T_c for carbon clathrates, relative to their silicon analogues.

3.4. Mulliken population analysis

Despite the fact that our main concern in this paper is the structure and equation of state for silicon clathrates and their carbon analogues, in this section we will briefly address the issue of electronic charge transference from the guest species to the host framework. This is a controversial issue, for which the literature offers contradictory results [11, 20, 54, 55]. The Mulliken population analysis for the isolated atoms and for the silicon and carbon clathrates studied in this work is summarized in table 9. The results were obtained within the HF-LCCO approximation, with C/Si 6-21G* split valence basis sets. As can be seen in table 9, our results indicate an almost complete charge transfer from the guest sodium atoms to the covalent framework for both Na_8C_{46} and Na_8Si_{46}. This is in excellent agreement with the recently published results from a full-potential linearized augmented-plane-wave (FLAPW) study of Na_8Si_{46} by Tse *et al* [11] and also with results from Moriguchi *et al* [20] and Ramachandran

Table 9. Mulliken charge and orbital population (in units of $|e|$) for the isolated atoms and for the clathrate compounds studied in this work.

			Orbital population				
Compound	Atom	Net charge	1s	2sp	3sp	3d(C)/4sp(Na/Si)	3d(Si)
	C	0.000	1.998	1.454	2.548	0.000	
	Si	0.000	2.000	7.964	1.753	2.282	0.000
	Na	0.000	2.000	6.145	1.811	1.043	
C_{46}	C(1)	−0.015	1.997	1.801	2.158	0.059	
	C(2)	0.029	1.997	1.862	2.050	0.062	
	C(3)	−0.015	1.997	1.819	2.141	0.058	
Na_8C_{46}	C(1)	−0.116	1.997	1.709	2.349	0.061	
	C(2)	−0.117	1.997	1.776	2.282	0.063	
	C(3)	−0.186	1.997	1.709	2.427	0.053	
	Na(1)	0.917	2.000	6.160	1.374	0.549	
	Na(2)	0.867	2.000	6.151	1.375	0.607	
Si_{46}	Si(1)	0.012	2.000	7.966	1.858	2.097	0.067
	Si(2)	0.005	2.000	7.966	1.899	2.060	0.070
	Si(3)	−0.006	2.000	7.966	1.872	2.102	0.067
Na_8Si_{46}	Si(1)	−0.120	2.000	7.966	1.796	2.288	0.070
	Si(2)	−0.134	2.000	7.966	1.789	2.311	0.068
	Si(3)	−0.191	2.000	7.966	1.790	2.366	0.069
	Na(1)	0.932	2.000	6.140	1.415	0.514	
	Na(2)	0.932	2.000	6.138	1.418	0.513	

et al [54]. Furthermore, in the case of Na_8C_{46}, the charge transfer is more pronounced for Na(1) than for Na(2), as the former occupies the site in the centre of the smallest cage. For Na_8Si_{46}, however, the two crystallographically distinct sodium atoms contribute about the same amount of electronic charge to the silicon framework.

A comparison between the sodium-inserted clathrates and their empty-cage counterparts reveals that electronic charge transfer from the guest species is directed mainly to the carbon 3sp and silicon 4sp orbitals. Relative to the isolated atom, the main reduction in the sodium orbital population is observed for the outermost 3sp and 4sp orbitals. In table 10 we show how this electronic charge transference affects the degree of bond-overlap population between pairs of atoms in the silicon and carbon clathrates studied in this work. It is reasonable to suppose that the degree of bond overlap could be of some importance in determining the rigidity of the covalent framework. Despite the increase in the total electronic charge for the whole set of framework atoms, the bond overlap in Na_8Si_{46} increases only for the Si(3)–Si(3) bonds, diminishing for all of the remaining silicon bonds. The situation is also similar for Na_8C_{46}: while the bond overlap increases, after sodium insertion, for C(1)–C(3) and C(2)–C(2), it decreases for the remaining C(2)–C(3) and C(3)–C(3) bonds. In fact, for the sodium-inserted carbon clathrate, the bond overlap C(3)–C(3) is almost the same as that found for the Si(3)–Si(3) bond in Na_8Si_{46}. In contrast, the C(2)–C(2) bond overlap in Na_8C_{46} increases by about 20%

Table 10. Interatomic distances and Mulliken bond overlap population (in units of $|e|$) for the clathrates C_{46}, Na_8C_{46}, Si_{46}, and Na_8Si_{46}.

Compound	Atom A	Atom B	d_{A-B} (Å)	AB bond overlap
C_{46}	C(1)	C(3)	1.569	0.373
	C(2)	C(2)	1.518	0.392
	C(2)	C(3)	1.540	0.378
	C(3)	C(3)	1.592	0.368
Na_8C_{46}	C(1)	C(3)	1.614	0.382
	C(2)	C(2)	1.504	0.471
	C(2)	C(3)	1.601	0.357
	C(3)	C(3)	1.733	0.320
	Na(1)	C(2)	2.261	−0.005
	Na(1)	C(3)	2.292	−0.003
	Na(2)	C(1)	2.460	−0.001
	Na(2)	C(2)	2.573	0.003
	Na(2)	C(3)	2.641	0.002
	Na(2)	C(3)	2.371	0.000
Si_{46}	Si(1)	Si(3)	2.404	0.308
	Si(2)	Si(2)	2.352	0.317
	Si(2)	Si(3)	2.373	0.306
	Si(3)	Si(3)	2.416	0.301
Na_8Si_{46}	Si(1)	Si(3)	2.385	0.281
	Si(2)	Si(2)	2.381	0.297
	Si(2)	Si(3)	2.386	0.290
	Si(3)	Si(3)	2.380	0.331
	Na(1)	Si(2)	3.252	0.003
	Na(1)	Si(3)	3.396	0.001
	Na(2)	Si(1)	3.627	0.001
	Na(2)	Si(2)	3.818	0.001
	Na(2)	Si(3)	3.434	0.004

relative to the empty clathrate, following the reduction by 0.97% in bond length after sodium insertion (the C(2)–C(2) distance is reduced by sodium insertion, despite an overall increase in bonding distances owing to the greater lattice parameter). As can be seen in table 10, the insertion of sodium in Na_8C_{46} does not promote a generalized increase in the C–C bond-overlap population. Only in the case of the C(2)–C(2) bonds, in the C_{24} cages, does the bond overlap increase significantly upon sodium insertion, which can effectively augment the rigidity of this C–C bond, relative to the empty clathrate C_{46}.

Figure 4 represents electronic charge-density difference maps for the clathrates C_{46}, Na_8C_{46}, and $Na_2Ba_6C_{46}$, as viewed along the normal to the plane that crosses the hexagonal bottleneck between two adjacent C_{24} cages. For the clathrate C_{46}, at the top of the figure, one can see the charge build-up at the mid-point of the covalent bonds along the edges of the hexagonal bottleneck. These bonds, however, become more and more diffuse, particularly the C(3)–C(3) bonds, in going from C_{46} (figure 4(a)) to the sodium-inserted Na_8C_{46} (figure 4(b)) and to $Na_2Ba_6C_{46}$ (figure 4(c)), mainly because of lattice expansion. In the latter compound, the C(3)–C(3) bond is broken, leaving highly reactive dangling bonds at each one of the C(3) atoms.

The small bond overlap between guest atoms and the host framework (as quoted in table 10), and the electronic charge-density difference maps (figure 4), both suggest an insignificant degree of covalence in the interaction between sodium atoms and the silicon/carbon framework for Na_8Si_{46} and Na_8C_{46}, in accordance with previous results obtained by Tse *et al* [11].

4. Conclusions

In this paper we discussed the effect of substituting carbon for silicon on the structure and equation of state for some type-I clathrate compounds, and also how the structure and bulk modulus for these compounds are influenced by the insertion of guest atoms into the clathrate cages. It was shown that the insertion of sodium into the carbon clathrate C_{46} leads to a volume increase not observed in the case of the analogous silicon compound. Furthermore, large guest species, such as barium, cannot be inserted in type-I carbon clathrates, even within the larger C_{24} cages, without C–C bond breaking. Early expectations about carbon clathrates less compressible than diamond were not confirmed by our calculations. In fact, for all of the carbon analogues of type-I silicon clathrates studied in this work, the calculated bulk moduli were always smaller than that of diamond, as a result of the greater volume per atom, relative to the diamond phase. In spite of that, the estimated hardness for C_{46}, $H = 61$ GPa, indicates that this compound, once prepared, would be the second-hardest material known, halfway in hardness between c-BN and diamond. From the calculated enthalpy for the diamond and clathrate phases, it was found that carbon clathrates C_{46} and Na_8C_{46} are stable, relative to the diamond phase, only at very negative pressures, which can help one to understand why, thirty-five years after the preparation of the first silicon clathrates, the synthesis of their carbon analogues still remains a challenge to the experimentalists.

Regarding the bulk modulus of these compounds, our results suggest that the main deleterious effect of guest-atom insertion into the empty cages of carbon clathrates is the volume increase of the host framework. In fact, the bulk modulus of the empty clathrate C_{46} is higher among the carbon clathrates studied in this work. This is in accordance with early studies that indicate that the main factor contributing to the high bulk modulus of diamond-like materials is the short bond length [52]. Accordingly, it can be supposed that a good recipe for the obtaining of carbon clathrates with high bulk modulus and hardness similar (or even superior) to that of diamond is the insertion of small guest species, like lithium or helium,

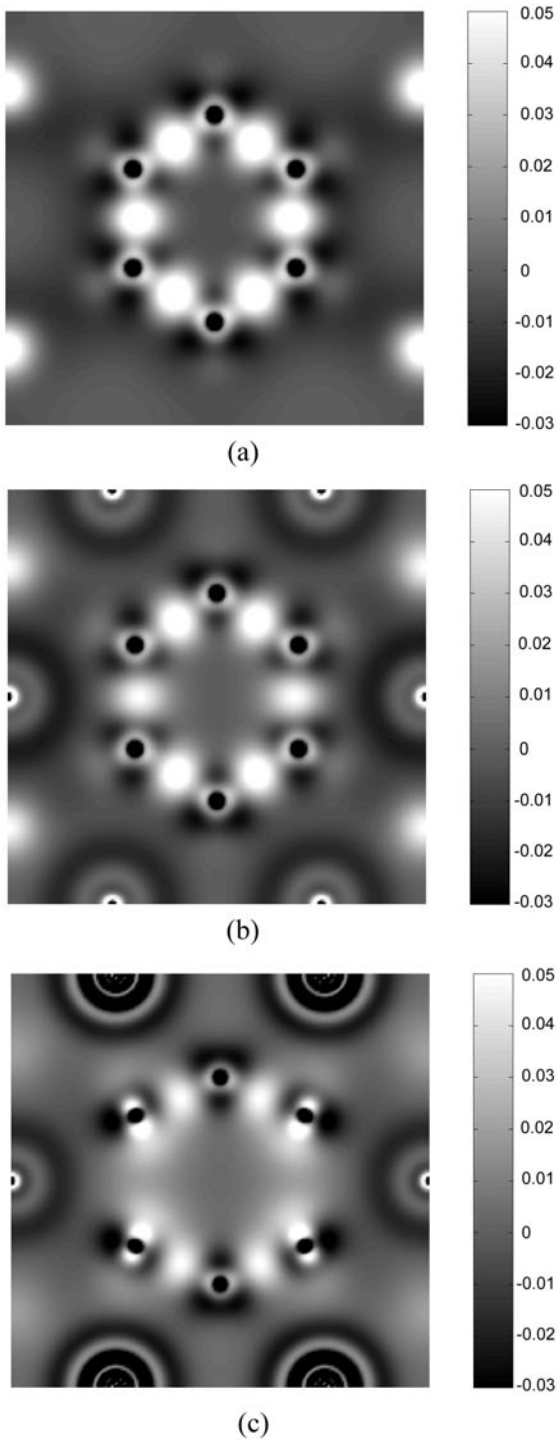

Figure 4. Electronic charge-density difference maps (in au) for (a) C_{46}, (b) Na_8C_{46}, and (c) $Na_2Ba_6C_{46}$, viewed normal to the plane along the hexagonal bottleneck formed by the shared face between two adjacent C_{24} cages.

which could even help to increase the stability of the clathrate structure [19, 21]. These guest atoms should have ionic (or atomic) radii such that they could fit inside the clathrate cages with no need for volume increase of the covalent carbon framework. By fulfilling this condition, upon pressure increase, the lattice compression would be opposed by short-range repulsion between the guest species and the framework atoms, thus leading to a bulk modulus higher than that of the empty-cage clathrate. It remains as open question whether this recipe can effectively lead to carbon clathrates less compressible than diamond and also whether these hypothetical carbon compounds could someday be synthesized at last.

Acknowledgments

The authors would like to thank Dr A S Pereira for fruitful discussions. The *ab initio* calculations described in this paper were carried out at the Centro Nacional de Supercomputação—CESUP, Porto Alegre, RS (Brazil). This work was supported by PRONEX/CNPq, FINEP and FAPERGS (Brazil).

References

[1] Powell H M 1948 *J. Chem. Soc.* **61**
[2] Hagan M 1962 *Clathrate Inclusion Compounds* (London: Reinhold)
[3] Cros C 1990 The formation of clathrates *Inorganic Reactions and Methods* vol 17, ed J J Zuckerman and A P Hagen (New York: VCH) p 209
[4] Müller A, Reuter H and Dillinger S 1995 *Angew. Chem. Int. Edn Engl.* **34** 2328
[5] Cros C, Pouchard M and Hagenmuller P 1965 *C. R. Acad. Sci., Paris* **260** 4764
[6] Kasper J S, Hagenmuller P, Pouchard M and Cros C 1965 *Science* **150** 1713
[7] Kawaji H, Horie H, Yamanaka S and Ishikawa M 1995 *Phys. Rev. Lett.* **74** 1427
[8] Yamanaka S, Horie H, Kawaji H and Ishikawa M 1995 *Eur. J. Solid State Inorg. Chem.* **32** 799
[9] Bryan J D, Srdanov V I, Stucky G D and Schmidt D 1999 *Phys. Rev.* B **60** 3064
[10] Iversen B *et al* 2000 *J. Solid State Chem.* **149** 455
[11] Tse J S, Uehara K, Rousseau R, Ker A and Ratcliffe C I 2000 *Phys. Rev. Lett.* **85** 114
[12] Nolas G S, Weakley T J R, Cohn J L and Sharma R 2000 *Phys. Rev.* B **61** 3845
[13] Dong J, Sankey O F, Ramachandran G K and McMillan P F 2000 *J. Appl. Phys.* **87** 7726
[14] Nolas G S, Cohn J L, Slack G A and Schujman S B 1998 *Appl. Phys. Lett.* **73** 178
[15] Blake N P, Mollnitz L, Kresse G and Metiu H 1999 *J. Chem. Phys.* **111** 3133
[16] Benedek G, Galvani E and Sanguinetti S 1995 *Nuovo Cimento* D **17** 97
[17] Yamanaka S, Horie H, Nakano H and Ishikawa M 1995 *Fullerene Sci. Technol.* **3** 21
[18] Saito S and Oshiyama A 1995 *Phys. Rev.* B **51** 2628
[19] San-Miguel A *et al* 1999 *Phys. Rev. Lett.* **83** 5290
[20] Moriguchi K, Yonemura M, Shintani A and Yamanaka S 2000 *Phys. Rev.* B **61** 9859
[21] Bernasconi M, Gaito S and Benedek G 2000 *Phys. Rev.* B **61** 12 689
[22] Saito S 1997 *Proc. 1st Symp. on Atomic-Scale Surface and Interface Dynamics (Tokyo)* p 47
[23] Sekkal W, Abderahmane S A, Terki R, Certier M and Aourag H 1999 *Mater. Sci. Eng.* B **64** 123
[24] Benedek G, Galvani E, Sanguinetti S and Serra S 1995 *Chem. Phys. Lett.* **244** 339
[25] Nesper R, Vogel K and Blöchl P E 1993 *Angew. Chem. Int. Edn Engl.* **32** 701
[26] Adams G B, O'Keefe M, Demkov A A, Sankey O F and Huang Y M 1994 *Phys. Rev.* B **49** 8048
[27] Menon M, Richter E and Subbaswamy K R 1997 *Phys. Rev.* B **56** 12 290
[28] Kahn D and Lu J P 1997 *Phys. Rev.* B **56** 13 898
[29] O'Keefe M, Adams G B and Sankey O F 1998 *Phil. Mag. Lett.* **78** 21
[30] Clerc D G J 1998 *Mater. Sci. Lett.* **17** 1461
[31] Dovesi R, Saunders V R, Roetti C, Causà M, Harrison N M, Orlando R and Aprà E 1996 *CRYSTAL95 User's Manual* University of Torino
[32] Perdew J P, Burke K and Ernzerhof M 1996 *Phys. Rev. Lett.* **77** 3865
[33] Binkley J S, Pople J A and Hehre W J 1980 *J. Am. Chem. Soc.* **102** 939
[34] Gordon M S, Binkley J S, Pople J A, Pietro W J and Hehre W J 1982 *J. Am. Chem. Soc.* **104** 2797
[35] Prencipe M, Zupan A, Dovesi R, Aprà E and Saunders V R 1995 *Phys. Rev.* B **51** 3391

[36] Towler M, unpublished results (http://www.tcm.phy.cam.ac.uk/ ˜mdt26/ basis_sets/Ba_basis.txt)
[37] Monkhorst H J and Pack J D 1976 *Phys. Rev.* B **13** 5188
[38] Gilat G and Raubenheimer J L 1966 *Phys. Rev.* **144** 390
[39] Bettinger H F, Schleyer P von R and Schaefer H F III 1998 *Chem. Commun.* **7** 769
[40] Murnaghan F D 1944 *Proc. Natl Acad. Sci. USA* **50** 697
[41] Gillet P, Fiquet G, Daniel I and Reynard B 1999 *Phys. Rev.* B **60** 14 660
[42] Okada Y and Tokumaru Y 1984 *J. Appl. Phys.* **56** 314
[43] Hu J Z and Spain I L 1984 *Solid State Commun.* **51** 263
[44] Orlando R, Dovesi R, Roetti C and Saunders V R 1990 *J. Phys.: Condens. Matter* **2** 7769
[45] Catti M, Freyria Fava F, Zicovich C and Dovesi R 1999 *Phys. Chem. Minerals* **26** 389
[46] Adams G B, Sankey O F, Page J B, O'Keefe M and Drabold D A 1992 *Science* **256** 1792
[47] Dong J and Sankey O 1999 *J. Phys.: Condens. Matter* **11** 6129
[48] Pandey R, Causà M, Harrison N M and Seel M 1996 *J. Phys.: Condens. Matter* **8** 3993
[49] Bundy F P, Bovenkerk H P, Strong H M and Wentorf R H Jr 1961 *J. Chem. Phys.* **35** 383
[50] Hashin Z and Shtrikman S 1962 *J. Mech. Phys. Solids* **10** 335
[51] Hashin Z and Shtrikman S 1962 *J. Mech. Phys. Solids* **10** 343
[52] Clerc D G 1999 *J. Phys. Chem. Solids* **60** 103
[53] Anderson O L 1963 *J. Phys. Chem. Solids* **24** 909
[54] Ramachandran G K, McMillan P F, Diefenbacher J, Dong J and Sankey O F 1999 *Phys. Rev.* B **60** 12 294
[55] Brunet F *et al* 2000 *Phys. Rev.* B **61** 16 550